Available online at www.sciencedirect.com
SCIENCE DIRECT®
International Journal of Solids and Structures 41 (2004) 7399–7422
INTERNATIONAL JOURNAL OF SOLIDS and STRUCTURES
www.elsevier.com/locate/ijsolstr

Generalized continuum modeling of 2-D periodic cellular solids

Rajesh S. Kumar *, David L. McDowell

G.W. Woodruff School of Mechanical Engineering, Georgia Institute of Technology, Atlanta, GA 30332-0405, USA

Received 4 February 2004; received in revised form 15 June 2004
Available online 12 August 2004

Abstract

A generalized continuum representation of two-dimensional periodic cellular solids is obtained by treating these materials as micropolar continua. Linear elastic micropolar constants are obtained using an energy approach for square, equilateral triangular, mixed triangle and diamond cell topologies. The constants are obtained by equating two different continuous approximations of the strain energy function. Furthermore, the effects of shear deformation of the cell walls on the micropolar elastic constants are also discussed. A continuum micropolar finite element approach is developed for numerical simulations of the cell structures. The solutions from the continuum representation are compared with the "exact" discrete simulations of these cell structures for a model problem of elastic indentation of a rectangular domain by a point force. The utility of the micropolar continuum representation is illustrated by comparing various cell structures with respect to the stress concentration factor at the root of a circular notch.

Keywords: Generalized continuum; Micropolar; Cosserat; Cellular solid; Discrete modeling; Finite elements

1. Introduction

Cellular solids are found in many natural and man-made structures. Cancellous or trabecular bone, wood, cork and honeycomb of bees are familiar natural cellular materials. Man-made cellular solids are found in a variety of structures such as sandwich panels, cushioning foams, compact heat exchangers, heat resistant ceramic tiles of space shuttles and artificial biological implants. It is well known that cellular materials can extend the range of properties achievable by their solid counterparts (Gibson and Ashby, 1997). In the last decade, cellular materials have emerged as promising multifunctional material systems (Evans et al.,

* Corresponding author. Tel.: +1 404 894 8495; fax: +1 404 894 0186.
E-mail addresses: rajesh.kumar@me.gatech.edu (R.S. Kumar), david.mcdowell@me.gatech.edu (D.L. McDowell).

0020-7683/$ - see front matter © 2004 Elsevier Ltd. All rights reserved.
doi:10.1016/j.ijsolstr.2004.06.038

1998, 2001). Specifically, 2-D prismatic cellular metals or metal honeycombs have a combination of properties that make them suitable for a range of applications such as ultra-light-weight structures, heat exchangers, energy absorption systems, vibration control and acoustical scattering. In many applications, the material is required to meet multiple performance objectives. For example, it may be required to carry mechanical loads as well as to serve as a heat sink. Metal honeycombs are manufactured using a powder slurry extrusion process developed at the Georgia Institute of Technology and are known as linear cellular alloys (LCAs) (Cochran et al., 2000). This manufacturing process allows complex cell arrangements and shapes to be fabricated at fine scale if necessary and hence provides a tremendous opportunity to tailor these materials for a given multifunctional application.

Mechanical behavior of cellular solids has been extensively studied. Gibson and co-workers have studied the elastic stiffness, elastic buckling, plastic collapse and brittle fracture of 2-D honeycombs and 3-D foams. These results are summarized in the book by Gibson and Ashby (1997). Recently, Wang and McDowell (2004, in press) have derived the elastic and plastic properties of 2-D cellular structures of various topologies. In all these works, the overall properties are evaluated via discrete modeling in which the individual cell walls are modeled as beams or struts. For uniform cell structures, analytical solutions are obtained by analyzing a periodic unit cell, whereas for non-uniform cell structures, computational analyses have been used.

While discrete analyses of cellular structures give very accurate stresses and strains in the cell walls, they are computationally expensive. Furthermore, in many applications, such accurate distributions of stresses and strains are not needed. For example, in a design exercise in which various 2-D cellular materials are to be rank-ordered with respect to, say, fracture toughness or notch resistance, it is prudent to represent the cellular material as an equivalent continuum as an alternative to discrete modeling of cellular structures. Banks and Sokolowski (1968) developed an analogy between rectangular lattice and couple stress theory. The couple stress theory is equivalent to the reduced Cosserat theory (Cosserat and Cosserat, 1909), in which rotations are obtained from the anti-symmetric part of the displacement gradient tensor. Askar and Cakmak (1968) obtained micropolar representation of a rectangular lattice with diagonals. Micropolar theory, developed by Eringen (1966), introduces independent rotations in addition to displacement fields and is equivalent to full Cosserat theory (Cosserat and Cosserat, 1909). Bazant (1971) and Bazant and Christensen (1972) derived the micropolar constants for a rectangular lattice by including higher order terms in the strain energy approximation. They also considered the effect of initial stresses and buckling. Perano (1983) also obtained micropolar elastic constants for discrete structures using the energy approach. More recently, Chen et al. (1998) have studied the brittle fracture of cellular materials by representing the cellular microstructure by an equivalent micropolar medium. They have analyzed square, triangular and regular hexagonal cell structures with respect to their fracture resistance.

The approach adopted in the aforementioned works is based on equating the continuum approximation of the strain energy of the discrete structure to the strain energy of an equivalent micropolar continuum. Except for Bazant (1971) and Bazant and Christensen (1972), all the remaining works consider only the first order derivatives in the Taylor series expansion of the displacement and rotation fields to achieve the continuum approximation of the strain energy density function. Bazant (1971) and Bazant and Christensen (1972) have retained the first order derivatives as well as those second order derivative terms that can be converted into first order by integration by parts. They show that this approach is necessary to describe joint equilibrium. The procedure of retaining the second order derivatives and then integrating by parts leads to different micropolar constants than those obtained by ignoring the second order terms. Specifically, the constants relating the in-plane moments and curvature are different for the two approaches, whereas the constants relating the stresses to strains are exactly the same. An alternative to the energy approach has been adopted by some researchers in deriving the micropolar constants of 2-D cellular structures, in which joint equilibrium as well as compatibility of displacement and micro-rotation are satisfied exactly by

considering a structural analysis of a representative unit cell (Wang and Stronge, 1999; Warren and Byskov, 2002).

The goal of this paper is to derive micropolar constants for a range of periodic 2-D honeycomb cell topologies, including rectangle, equilateral triangle, mixed square-triangle and diamond. The cell structures considered in this paper are restricted to those for which a periodic unit cell containing a single joint can be identified. Two prominent cell topologies that violate this requirement are hexagonal and Kagome. Hexagonal cell structures contain two different types of joints—for one the cell walls meet at 0°, 120° and 240° angles and for the other the cell walls meet at 60°, 180° and 300° angles with respect to horizontal. On the other hand, the Kagome cell structure contains three different types of joints. For both these structures a periodic unit cell must contain more than one joint. Furthermore, the joints are not located at the centroid of the unit cell. To obtain the micropolar elastic constants for these cell topologies either explicit structural analysis of the unit cell, as presented in Warren and Byskov (2002), or an extended energy approach with explicit enforcement of equilibrium at the joints may be needed (Kumar and McDowell, in preparation).

The constants are obtained using an energy approach similar to those adopted in previous works (Bazant and Christensen, 1972; Chen et al., 1998). In deriving the micropolar constants, the cell walls are treated as both Euler–Bernoulli beams and Timoshenko beams. Two sets of constants are derived for each of these two cases: one set retaining the second order derivatives in the strain energy approximation and the other set ignoring it. The issue of negative micropolar constants as obtained by the former approach is discussed. A two-dimensional micropolar finite element is developed to compare the prediction of micropolar theory with different sets of constants with "exact" discrete analysis. The usefulness of generalized continuum modeling of cellular materials is then illustrated by comparing different cell topologies with respect to (i) elastic indentation of a rectangular domain, and (ii) the stress concentration factor at the root of circular notch.

2. Generalized continuum representation—micropolar elasticity

The in-plane deformation of 2-D honeycombs is characterized by cell wall stretching and cell wall bending (Deshpande et al., 2001). In addition, the joints can translate in the plane as well as rotate about an axis normal to the plane (Fig. 1). It is clear from Fig. 1 that the total rotation at a joint consists of macroscopic

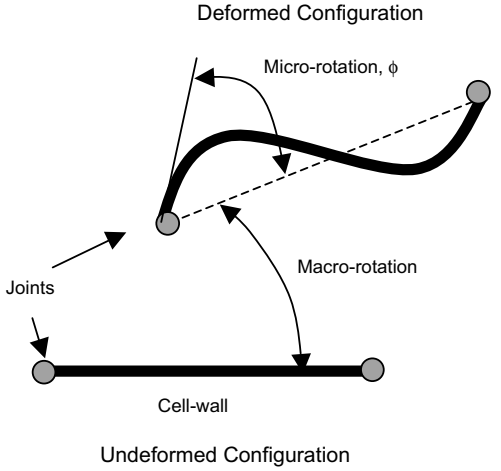

Fig. 1. In-plane deformation of a typical cell-wall.

rotation associated with cell wall rotation and a microscopic rotation associated with the joint rotation. Furthermore these two rotations are independent of each other—the macroscopic rotation is associated with the translation of the joints and the microscopic rotation is an independent joint rotation. Thus in order to represent the linear cellular material as an equivalent continuum, we must consider a micropolar continuum that allows for independent rotational degree of freedom.

In the classical theory of continuum mechanics, each material point has translational degrees of freedom. Furthermore, the interaction between two neighboring material points is via stress traction and the theory is local. In order to capture limited non-locality, the classical theory has been enriched by adding independent rotational degrees of freedom at each material point. This theory is referred to as Cosserat or micropolar theory (see Nowacki, 1986). In the micropolar theory, the material point support couple stresses in addition to the usual Cauchy-type stress; however, micropolar theory differs from the couple stress theory or the reduced Cosserat theory in which the rotational degree of freedom is not independent, being obtained from the anti-symmetric part of the displacement gradient tensor.

We restrict our attention here to infinitesimal strains and rotations. The governing equations of linear micropolar elasticity (Eringen, 1966, 1968, 1999; Nowacki, 1986) are given by balance of linear momentum, i.e.,

$$\sigma_{ji,j} + f_i = 0 \tag{1}$$

and balance of moment of momentum, i.e.,

$$e_{ijk}\sigma_{jk} + m_{ji,j} + g_i = 0 \tag{2}$$

The kinematic relations are given by

$$\varepsilon_{ji} = u_{i,j} - e_{kji}\phi_k \tag{3}$$

$$\kappa_{ji} = \phi_{i,j} \tag{4}$$

Finally, the constitutive equations are listed as

$$\sigma_{ji} = A_{jikl}\varepsilon_{kl} + B_{jikl}\kappa_{kl} \tag{5}$$

$$m_{ji} = B_{klji}\varepsilon_{kl} + C_{jikl}\kappa_{kl} \tag{6}$$

These are supplemented by displacement and micro-rotation boundary conditions,

$$\begin{aligned} u_i &= u_i^{\mathrm{P}} \\ \phi_i &= \phi_i^{\mathrm{P}} \end{aligned} \tag{7}$$

as well as traction boundary conditions, given by

$$\begin{aligned} \sigma_{ji}n_j &= t_i^{\mathrm{P}} \\ m_{ji}n_j &= c_i^{\mathrm{P}} \end{aligned} \tag{8}$$

Here, σ_{ij} is the non-symmetric stress tensor, m_{ij} is the couple stress tensor, f_i is the applied body force, g_i is the applied body moment, ε_{ij} is the strain tensor, ϕ_i is the micro-rotation vector, and κ_{ij} is the curvature tensor. The prescribed value of displacement, micro-rotation, stress traction and couple stress traction are denoted by u_i^{P}, ϕ_i^{P}, t_i^{P} and c_i^{P}, respectively, defined on the boundary with an outward unit normal vector n_i. The constitutive behavior is described by fourth rank tensors $\boldsymbol{A}$, $\boldsymbol{B}$, and $\boldsymbol{C}$. The uniform periodic cell structures considered here are centrally symmetric and hence the components of the coupling term in the constitutive description, B_{ijkl}, are identically zero.

In 2-D plane deformation of a micropolar solid, at each material point there are two displacement components, u_1 and u_2, and one rotational degree of freedom, $\phi(=\phi_3)$. The generalized strain vector, which

includes strains and curvatures, is related to the displacement gradients, micro-rotation and micro-rotation gradients (using Eqs. (3) and (4)) by

$$\{\varepsilon\} = \begin{Bmatrix} \varepsilon_{11} \\ \varepsilon_{22} \\ \varepsilon_{12} \\ \varepsilon_{21} \\ \kappa_{13} \\ \kappa_{23} \end{Bmatrix} = \begin{Bmatrix} u_{1,1} \\ u_{2,2} \\ u_{2,1} - \phi \\ u_{1,2} + \phi \\ \phi_{,1} \\ \phi_{,2} \end{Bmatrix} \tag{9}$$

where we have abbreviated $\phi = \phi_3$, $\phi_{,1} = \phi_{3,1}$ and $\phi_{,2} = \phi_{3,2}$. The corresponding generalized stress vector is given by

$$\{\sigma\} = [\, \sigma_{11} \quad \sigma_{22} \quad \sigma_{12} \quad \sigma_{21} \quad m_{13} \quad m_{23} \,]^{\mathrm{T}} \tag{10}$$

Using these stress and strain components, the constitutive equations (Eqs. (5) and (6)) can be written as

$$\{\sigma\} = [D]\{\varepsilon\} \tag{11}$$

where $[D]$ is the 6×6 matrix of constitutive law coefficients.

The strain energy density of the micropolar elastic continuum can be written as a function of displacement gradients, micro-rotation, and micro-rotation gradients, i.e.,

$$w = w(\varepsilon_{11}, \varepsilon_{22}, \varepsilon_{12}, \varepsilon_{21}, \kappa_{13}, \kappa_{23}) = w(u_{1,1}, u_{2,2}, (u_{2,1} - \phi), (u_{1,2} + \phi), \phi_{,1}, \phi_{,2}) \tag{12}$$

with additional possible dependence on higher order gradient terms of the micro-rotation field. The stresses and couple stresses are derived from the strain energy density function, w, i.e.,

$$\sigma_{11} = \frac{\partial w}{\partial \varepsilon_{11}} = \frac{\partial w}{\partial u_{1,1}}, \qquad \sigma_{22} = \frac{\partial w}{\partial \varepsilon_{22}} = \frac{\partial w}{\partial u_{2,2}} \tag{13}$$

$$\sigma_{12} = \frac{\partial w}{\partial \varepsilon_{12}} = \frac{\partial w}{\partial (u_{2,1} - \phi)}, \qquad \sigma_{21} = \frac{\partial w}{\partial \varepsilon_{21}} = \frac{\partial w}{\partial (u_{1,2} + \phi)} \tag{14}$$

$$m_{13} = \frac{\partial w}{\partial \kappa_{13}} = \frac{\partial w}{\partial \phi_{,1}}, \qquad m_{23} = \frac{\partial w}{\partial \kappa_{23}} = \frac{\partial w}{\partial \phi_{,2}} \tag{15}$$

In order to obtain the micropolar constitutive matrix, $[D]$, for various periodic cell structures, we must obtain the continuum approximation of the strain energy (Eq. (12)) for each of them by analyzing a representative periodic unit cell. This is discussed in the next section.

3. Continuum approximation of elastic strain energy

In order to obtain the continuum approximation of the strain energy for different periodic cell structures, we need to first identify an appropriate unit cell of the discrete structure. The strain energy of the discrete structure is calculated by summing the contribution from strain energies of the individual members of the cell. This strain energy is expressed in terms of displacements and rotations of joints. The continuum approximation is then obtained by expressing the joint displacement and rotation in terms of displacement and rotation of the centroid of the unit cell using a Taylor series expansion.

To illustrate the approach, consider a typical member of the 2-D prismatic cell structure between two adjacent joints I and J shown in Fig. 2. In the initial undeformed state, the member is inclined at

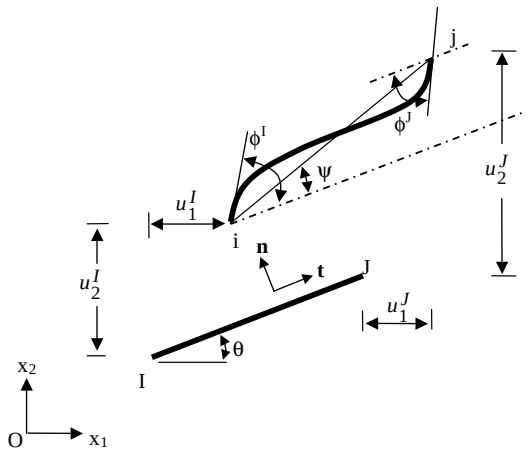

Fig. 2. Initial and deformed geometry of a typical cell wall member of the cellular solid.

an angle θ (measured counterclockwise) with respect to the global x_1-axis. Let $\boldsymbol{n}$ and $\boldsymbol{t}$ be the unit normal and unit tangential vectors, respectively, to the initial cell wall. After deformation, the member is in the position i–j (see Fig. 2) with joint displacements $\boldsymbol{u}^{\mathrm{I}}$ and $\boldsymbol{u}^{\mathrm{J}}$. Furthermore, joints I and J rotate by angle ϕ^{I} and ϕ^{J}, respectively. These rotations are with respect to the initial configuration and are considered positive counterclockwise.

Considering small deformation and neglecting the shear deformation of the beam, the total strain energy per unit width of the cell wall in member I–J is given by the summing the contribution due to axial and bending deformation, i.e.,

$$W^{\mathrm{IJ}} = \frac{E'}{2}\begin{bmatrix} u_t^{\mathrm{I}} & u_t^{\mathrm{J}} \end{bmatrix}\begin{bmatrix} 1 & -1 \\ -1 & 1 \end{bmatrix}\begin{Bmatrix} u_t^{\mathrm{I}} \\ u_t^{\mathrm{J}} \end{Bmatrix} + \frac{k}{2}\begin{bmatrix} u_n^{\mathrm{I}} & \phi^{\mathrm{I}} & u_n^{\mathrm{J}} & \phi^{\mathrm{J}} \end{bmatrix}\begin{bmatrix} s''/L^2 & s'/L & -s''/L^2 & s'/L \\ s'/L & s & -s'/L & sc \\ -s''/L^2 & -s'/L & s''/L^2 & -s'/L \\ s'/L & sc & -s'/L & s \end{bmatrix}\begin{Bmatrix} u_n^{\mathrm{I}} \\ \phi^{\mathrm{I}} \\ u_n^{\mathrm{J}} \\ \phi^{\mathrm{J}} \end{Bmatrix} \tag{16}$$

where u_n and u_t are components of displacement along the normal ($\boldsymbol{n}$) and tangential ($\boldsymbol{t}$) directions, respectively; $E' = Eh/L$; $k = Eh^3/(12L)$; L and h are the length and the thickness of the member, respectively. For plane strain analysis, $E = E_{\mathrm{s}}/(1-\nu_{\mathrm{s}}^2)$; for plane stress, $E = E_{\mathrm{s}}$. Here E_{s} is the modulus of elasticity and ν_{s} is the Poisson's ratio of the solid cell wall material. For the case of zero initial axial forces, the stability functions s and c are simply 4 and 1/2, respectively, and $s' = s(1+c)$, $s'' = 2s'$.

In Eq. (16), the strain energy of the member is expressed in terms of the joint displacements and micro-rotations. In order to obtain the continuum field approximation, we assume that the displacements and micro-rotations at joints I and J can be approximated by a second order Taylor series expansion of the corresponding kinematic variables at the origin of the unit cell located at point O. This origin need not coincide with any joint in the structure. Of course our assumption is that the variation in the kinematic quantities from joint to joint is smooth. Thus, the displacement vector and joint rotation at I and J are expanded as

$$\boldsymbol{u}^{\mathrm{I}} = \boldsymbol{u} + L_{\mathrm{OI}}\frac{\partial \boldsymbol{u}}{\partial t_{\mathrm{OI}}} + \frac{L_{\mathrm{OI}}^2}{2}\frac{\partial^2 \boldsymbol{u}}{\partial t_{\mathrm{OI}}^2} + \cdots \tag{17}$$

$$\phi^{\mathrm{I}} = \phi + L_{\mathrm{OI}}\frac{\partial \phi}{\partial t_{\mathrm{OI}}} + \frac{L_{\mathrm{OI}}^2}{2}\frac{\partial^2 \phi}{\partial t_{\mathrm{OI}}^2} + \cdots \tag{18}$$

$$\boldsymbol{u}^{\mathrm{J}} = \boldsymbol{u} + L_{\mathrm{OJ}}\frac{\partial \boldsymbol{u}}{\partial t_{\mathrm{OJ}}} + \frac{L_{\mathrm{OJ}}^2}{2}\frac{\partial^2 \boldsymbol{u}}{\partial t_{\mathrm{OJ}}^2} + \cdots \tag{19}$$

$$\phi^{\mathrm{J}} = \phi + L_{\mathrm{OJ}}\frac{\partial \phi}{\partial t_{\mathrm{OJ}}} + \frac{L_{\mathrm{OJ}}^2}{2}\frac{\partial^2 \phi}{\partial t_{\mathrm{OJ}}^2} + \cdots \tag{20}$$

where t_{OI} and t_{OJ} are the coordinates along the directions OI and OJ joining the origin O and joints I and J, respectively. The distance of joints I and J from the origin O is given by L_{OI} and L_{OJ}, respectively. The normal and tangential (to the cell wall) components of the displacement at the two joints are obtained using the following relations

$$u_n^{\mathrm{I}} = \boldsymbol{n}\cdot\boldsymbol{u}^{\mathrm{I}}; \qquad u_t^{\mathrm{I}} = \boldsymbol{t}\cdot\boldsymbol{u}^{\mathrm{I}} \tag{21}$$

$$u_n^{\mathrm{J}} = \boldsymbol{n}\cdot\boldsymbol{u}^{\mathrm{J}}; \qquad u_t^{\mathrm{J}} = \boldsymbol{t}\cdot\boldsymbol{u}^{\mathrm{J}} \tag{22}$$

Substituting these expressions in Eq. (16) gives a continuum field approximation of the strain energy of member IJ. The sum contribution of the strain energies of all the members of the representative unit cell of the cell structure gives the total strain energy. This is then divided by the planar area of the unit cell to obtain the strain energy density. The micropolar constitutive equations can then be obtained using Eqs. (13)–(15).

As mentioned in Section 1, another approximation is made before the strain energy function is derived to obtain the constitutive equations. In most of the approaches (cf. Chen et al., 1998), the second order derivative terms in the kinematic approximations are excluded. On the other hand, Bazant and Christensen (1972) advocate retaining terms of the form $\phi\phi_{,11}$ and $\phi\phi_{,22}$ as they can result in first order derivative terms by simple integration by parts. If such terms are retained, the strain energy density function can be written as the sum of that due to first order derivatives (w^1) and the additional second order derivative terms, i.e.,

$$w = w^1 + c_1\phi\phi_{,11} + c_2\phi\phi_{,22} \tag{23}$$

where c_1 and c_2 are constants. The total strain energy over the unit cell can be written as

$$W = \int_V (w^1 + c_1\phi\phi_{,11} + c_2\phi\phi_{,22})\,\mathrm{d}V \tag{24}$$

Integrating the second order terms by parts leads to

$$W = \int_V (w^1 - c_1\phi_{,1}^2 - c_2\phi_{,2}^2)\,\mathrm{d}V + \int_{\partial V} (c_1\phi\phi_{,1} + c_2\phi\phi_{,2})\,\mathrm{d}S \tag{25}$$

Neglecting the surface integral (Bazant and Christensen, 1972), the strain energy density function in this approach is given by the first order derivative terms plus two additional terms, i.e.,

$$w = w^1 - c_1\phi_{,1}^2 - c_2\phi_{,2}^2 \tag{26}$$

4. Micropolar constitutive relations for various 2-D cell structures

The micropolar elastic constants for various cell structures are obtained by determining the continuum approximation of the strain energy density for a typical joint in a periodic cell structure. A repeating unit cell is first isolated for each cell structure and the strain energy contribution of each member forming the repeating structure is determined using the procedure discussed in Section 3, assuming the plane strain

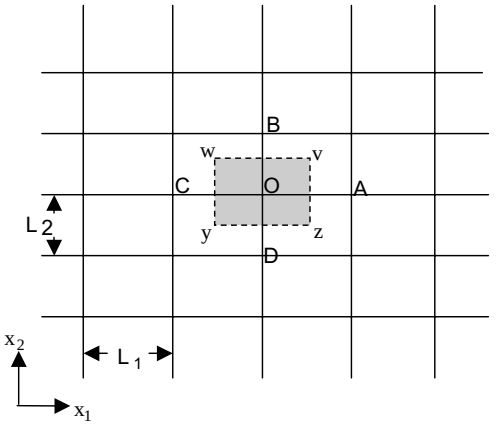

Fig. 3. Schematic of rectangular cell structure.

approximation. The components of stress and couple stress tensors are obtained using Eqs. (13)–(15). The procedure and the results for various cell structures are outlined below.

4.1. Rectangular and square cell structures

A schematic of the rectangular cell structure is shown in Fig. 3. The cell sizes in x_1 and x_2 directions are L_1 and L_2, respectively. The periodic unit cell is a rectangular region v–w–y–z.

The strain energy density (per unit depth in the x_3-direction) of the cell structure is calculated by determining the total strain energy stored in the repeating cell and dividing by its area. The strain energy of the unit cell is due to the deformation of members OA, OB, OC and OD. Thus, the strain energy density is given by

$$w = \frac{1}{2A_c}(W^{OA} + W^{OB} + W^{OC} + W^{OD}) \tag{27}$$

where A_c is the area of the unit cell given by

$$A_c = L_1 L_2 \tag{28}$$

In Eq. (27), a factor of half is due to the fact that each member at joint O contributes only half of its strain energy to the unit cell. To calculate individual terms of Eq. (27), we expand the displacement and micro-rotation at joints A, B, C and D in terms of their corresponding values at joint O. Let displacement at joint O be $\boldsymbol{u}$ and micro-rotation be ϕ. Then, displacement and micro-rotations at joints A, B, C, and D are given by

$$\begin{aligned}
\boldsymbol{u}^A &\approx \boldsymbol{u} + L_{OA}\frac{\partial \boldsymbol{u}}{\partial t_{OA}} + \frac{1}{2}L_{OA}^2\frac{\partial^2 \boldsymbol{u}}{\partial t_{OA}^2}; & \phi^A &\approx \phi + L_{OA}\frac{\partial \phi}{\partial t_{OA}} + \frac{1}{2}L_{OA}^2\frac{\partial^2 \phi}{\partial t_{OA}^2}\\
\boldsymbol{u}^B &\approx \boldsymbol{u} + L_{OB}\frac{\partial \boldsymbol{u}}{\partial t_{OB}} + \frac{1}{2}L_{OB}^2\frac{\partial^2 \boldsymbol{u}}{\partial t_{OB}^2}; & \phi^B &\approx \phi + L_{OB}\frac{\partial \phi}{\partial t_{OB}} + \frac{1}{2}L_{OB}^2\frac{\partial^2 \phi}{\partial t_{OB}^2}\\
\boldsymbol{u}^C &\approx \boldsymbol{u} + L_{OC}\frac{\partial \boldsymbol{u}}{\partial t_{OC}} + \frac{1}{2}L_{OC}^2\frac{\partial^2 \boldsymbol{u}}{\partial t_{OC}^2}; & \phi^C &\approx \phi + L_{OC}\frac{\partial \phi}{\partial t_{OC}} + \frac{1}{2}L_{OC}^2\frac{\partial^2 \phi}{\partial t_{OC}^2}\\
\boldsymbol{u}^D &\approx \boldsymbol{u} + L_{OD}\frac{\partial \boldsymbol{u}}{\partial t_{OD}} + \frac{1}{2}L_{OD}^2\frac{\partial^2 \boldsymbol{u}}{\partial t_{OD}^2}; & \phi^D &\approx \phi + L_{OD}\frac{\partial \phi}{\partial t_{OD}} + \frac{1}{2}L_{OD}^2\frac{\partial^2 \phi}{\partial t_{OD}^2}
\end{aligned} \tag{29}$$

where $L_{OA} = L_{OC} = L_1$, $L_{OB} = L_{OD} = L_2$ and

$$\frac{\partial}{\partial t_{OA}} = -\frac{\partial}{\partial t_{OC}} = \frac{\partial}{\partial x_1}; \qquad \frac{\partial}{\partial t_{OB}} = -\frac{\partial}{\partial t_{OD}} = \frac{\partial}{\partial x_2} \tag{30}$$

Substituting the kinematic variables from Eq. (29) in Eqs. (21) and (22), we obtain the normal and tangential components of displacement vector for each member of the unit cell. The total strain energy of each member is then obtained using Eq. (16). The resulting strain energy density, calculated using Eq. (27), is given by

$$\begin{aligned} w = \frac{1}{2L_1L_2}(&E_1'L_1^2u_{1,1}^2 + E_2'L_2^2u_{2,2}^2 + 12k_1(u_{2,1}-\phi)^2 + 12k_2(u_{1,2}+\phi)^2 + 4k_1L_1^2\phi_{,1}^2 + 4k_2L_2^2\phi_{,2}^2 \\ &+ 6k_1L_1^2\phi\phi_{,11} + 6k_2L_2^2\phi\phi_{,22}) \end{aligned} \tag{31}$$

Here partial derivative of a quantity $(\cdot)$ with respect to spatial coordinates x_1 and x_2 are indicated by $(\cdot)_{,1}$ and $(\cdot)_{,2}$ respectively and $E_i' = Eh/L_i$, $k_i = Eh^3/(12L_i)$, $i = 1, 2$. Note that only quadratic terms in the kinematic variables are retained. Furthermore, only the first order derivatives are retained except for the last two terms $6k_1L_1^2\phi\phi_{,11}$ and $6k_2L_2^2\phi\phi_{,22}$. As just discussed, they can be integrated by parts to contribute terms $-6k_1L_1^2\phi_{,1}^2$ and $-6k_2L_2^2\phi_{,2}^2$, respectively, to the total strain energy of the unit cell (see Eq. (26)). These terms are important in the strain energy density expression to maintain joint equilibrium as pointed out by Bazant (1971) and Bazant and Christensen (1972). However, these terms have been ignored in the recent works of Chen et al. (1998) and others. The expression for the strain energy density for this cell structure is given by

$$w = \frac{1}{2L_1L_2}(E_1'L_1^2u_{1,1}^2 + E_2'L_2^2u_{2,2}^2 + 12k_1(u_{2,1}-\phi)^2 + 12k_2(u_{1,2}+\phi)^2 - 2k_1L_1^2\phi_{,1}^2 - 2k_2L_2^2\phi_{,2}^2) \tag{32}$$

The micropolar constitutive equations are obtained by inserting Eq. (32) into Eqs. (13)–(15). The resulting relationships are given by

$$\begin{aligned} \sigma_{11} &= \frac{E_1'L_1}{L_2}\varepsilon_{11}, \qquad \sigma_{22} = \frac{E_2'L_2}{L_1}\varepsilon_{22} \\ \sigma_{12} &= \frac{12k_1}{L_1L_2}\varepsilon_{12}, \qquad \sigma_{21} = \frac{12k_2}{L_1L_2}\varepsilon_{21} \\ m_{13} &= -\frac{2k_1L_1}{L_2}\kappa_{13}, \qquad m_{23} = -\frac{2k_2L_2}{L_1}\kappa_{23} \end{aligned} \tag{33}$$

The above expressions are also valid for a square cell structure with $L_1 = L_2 = L$. In this case, $k_1 = k_2 = k$ and $E_1' = E_2' = E'$. For the square cell structure, the constitutive relations imply in-plane orthotropy, as expected.

If the higher order terms $6k_1L_1^2\phi\phi_{,11}$ and $6k_2L_2^2\phi\phi_{,22}$ are neglected in Eq. (31), the strain energy density is

$$w = \frac{1}{2L_1L_2}(E_1'L_1^2u_{1,1}^2 + E_2'L_2^2u_{2,2}^2 + 12k_1(u_{2,1}-\phi)^2 + 12k_2(u_{1,2}+\phi)^2 + 4k_1L_1^2\phi_{,1}^2 + 4k_2L_2^2\phi_{,2}^2) \tag{34}$$

The σ_{ij}–ε_{ij} relations remain same as in the previous case (Eq. (33)). However, the couple stress–curvature relations now become

$$m_{13} = \frac{4k_1L_1}{L_2}\kappa_{13}, \qquad m_{23} = \frac{4k_2L_2}{L_1}\kappa_{23} \tag{35}$$

4.2. Equilateral triangular cell structure

A schematic of the periodic equilateral triangular cell structure with a hexagonal repeating cell is shown in Fig. 4.

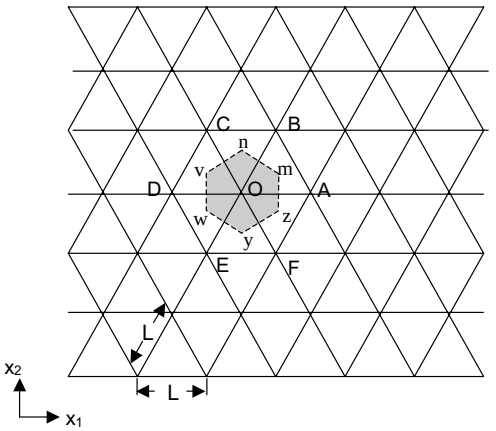

Fig. 4. Schematic of equilateral triangular cell structure.

It is clear from Fig. 4 that the strain energy density can be written as

$$w = \frac{1}{2A_c}\left(W^{OA} + W^{OB} + W^{OC} + W^{OD} + W^{OE} + W^{OF}\right) \tag{36}$$

where the area of the unit cell is $A_c = \sqrt{3}L^2/2$. We assign the displacement and micro-rotation of point O (centroid of the unit cell) as $\boldsymbol{u}$ and ϕ, respectively. Using Eqs. (17)–(20), the displacement and micro-rotation at surrounding joints are expanded in terms of a second order Taylor series expansion of the corresponding variables at O. For example, displacement and micro-rotation at joints A and B can be written as

$$\begin{aligned} \boldsymbol{u}^A &\approx \boldsymbol{u} + L_{OA}\frac{\partial \boldsymbol{u}}{\partial t_{OA}} + \frac{1}{2}L_{OA}^2\frac{\partial^2 \boldsymbol{u}}{\partial t_{OA}^2}; \qquad \phi^A \approx \phi + L_{OA}\frac{\partial \phi}{\partial t_{OA}} + \frac{1}{2}L_{OA}^2\frac{\partial^2 \phi}{\partial t_{OA}^2} \\ \boldsymbol{u}^B &\approx \boldsymbol{u} + L_{OB}\frac{\partial \boldsymbol{u}}{\partial t_{OB}} + \frac{1}{2}L_{OB}^2\frac{\partial^2 \boldsymbol{u}}{\partial t_{OB}^2}; \qquad \phi^B \approx \phi + L_{OB}\frac{\partial \phi}{\partial t_{OB}} + \frac{1}{2}L_{OB}^2\frac{\partial^2 \phi}{\partial t_{OB}^2} \end{aligned} \tag{37}$$

where $L_{OA} = L_{OB} = L$ and

$$\frac{\partial}{\partial t_{OA}} = \frac{\partial}{\partial x_1}; \qquad \frac{\partial}{\partial t_{OB}} = \frac{1}{2}\frac{\partial}{\partial x_1} + \frac{\sqrt{3}}{2}\frac{\partial}{\partial x_2} \tag{38}$$

Similar expressions are obtained for other joints. The normal and tangential components of displacement for each member are obtained using Eqs. (21) and (22) and the strain energy of each member is obtained using Eq. (16). The final expression for the strain energy density is obtained as

$$\begin{aligned} w = \frac{\sqrt{3}}{8L^2}\{&(3E'L^2 + 12k)u_{1,1}^2 + (3E'L^2 + 12k)u_{2,2}^2 + (2E'L^2 - 24k)u_{1,1}u_{2,2} + (E'L^2 + 36k)(u_{2,1} - \phi)^2 \\ &+ (E'L^2 + 36k)(u_{1,2} + \phi)^2 + (2E'L^2 - 24k)(u_{2,1} - \phi)(u_{1,2} + \phi) - 8kL^2\phi_{,1}^2 - 8kL^2\phi_{,2}^2\} \end{aligned} \tag{39}$$

Again only quadratic terms are retained. Further, all the terms that are second or higher order derivatives of the spatial coordinates are ignored except for those that can be converted in to a first order derivative using integration by parts, as discussed for the rectangular cell case.

Using Eq. (39) with Eqs. (13)–(15) gives

$$\begin{aligned}
\sigma_{11} &= \frac{\sqrt{3}}{4L^2}\{(3E'L^2 + 12k)\varepsilon_{11} + (E'L^2 - 12k)\varepsilon_{22}\} \\
\sigma_{22} &= \frac{\sqrt{3}}{4L^2}\{(E'L^2 - 12k)\varepsilon_{11} + (3E'L^2 + 12k)\varepsilon_{22}\} \\
\sigma_{12} &= \frac{\sqrt{3}}{4L^2}\{(E'L^2 + 36k)\varepsilon_{12} + (E'L^2 - 12k)\varepsilon_{21}\} \\
\sigma_{21} &= \frac{\sqrt{3}}{4L^2}\{(E'L^2 - 12k)\varepsilon_{12} + (E'L^2 + 36k)\varepsilon_{21}\} \\
m_{13} &= (-2\sqrt{3}k)\kappa_{13}, \qquad m_{23} = (-2\sqrt{3}k)\kappa_{23}
\end{aligned} \tag{40}$$

If the second order derivative terms are ignored, the constitutive relations remain same as Eq. (40) except the couple stress–curvature relations now become

$$m_{13} = (4\sqrt{3}k)\kappa_{13}, \qquad m_{23} = (4\sqrt{3}k)\kappa_{23} \tag{41}$$

4.3. Mixed triangle cell structure with square super lattice

We consider two mixed isosceles triangular cell structures which have a square super lattice. In mixed triangle A (Fig. 5), each square of size L has two diagonal members, whereas in mixed triangle B (Fig. 6), each square of size L has only one diagonal.

For mixed triangle A, the strain energy contribution from members OA, OC, OE, OG to the unit cell is half of their total strain energy, whereas, the contribution from members OB, OD, OF, OH is full. Thus,

$$w = \frac{1}{A_c}\left\{\frac{1}{2}(W^{OA} + W^{OC} + W^{OE} + W^{OG}) + W^{OB} + W^{OD} + W^{OF} + W^{OH}\right\} \tag{42}$$

where the area of the repeating cell is $A_c = L^2$. The strain energy density (retaining the second order derivative terms that can be integrated by parts to yield first order terms) in terms of kinematical variables is obtained as

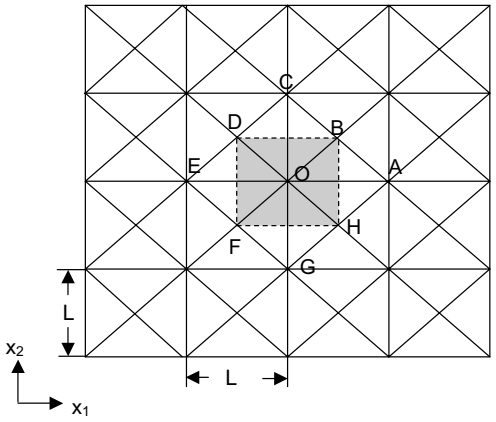

Fig. 5. Schematic of mixed triangular cell structure A.

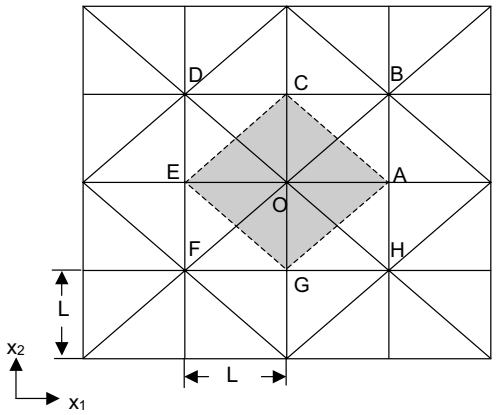

Fig. 6. Schematic of mixed triangular cell structure B.

$$w = \frac{1}{4L^2}\{(3E'L^2 + 24k)u_{1,1}^2 + (3E'L^2 + 24k)u_{2,2}^2 + (2E'L^2 - 48k)u_{1,1}u_{2,2} + (E'L^2 + 48k)(u_{2,1} - \phi)^2 + (E'L^2 + 48k)(u_{1,2} + \phi)^2 + (2E'L^2 - 48k)(u_{2,1} - \phi)(u_{1,2} + \phi) - 8kL^2\phi_{,1}^2 - 8kL^2\phi_{,2}^2\} \tag{43}$$

and the constitutive equations are derived from the strain energy as

$$\begin{aligned}
\sigma_{11} &= \frac{1}{2L^2}\{(3E'L^2 + 24k)\varepsilon_{11} + (E'L^2 - 24k)\varepsilon_{22}\} \\
\sigma_{22} &= \frac{1}{2L^2}\{(E'L^2 - 24k)\varepsilon_{11} + (3E'L^2 + 24k)\varepsilon_{22}\} \\
\sigma_{12} &= \frac{1}{2L^2}\{(E'L^2 + 48k)\varepsilon_{12} + (E'L^2 - 24k)\varepsilon_{21}\} \\
\sigma_{21} &= \frac{1}{2L^2}\{(E'L^2 - 24k)\varepsilon_{12} + (E'L^2 + 48k)\varepsilon_{21}\} \\
m_{13} &= (-4k)\kappa_{13}, \qquad m_{23} = (-4k)\kappa_{23}
\end{aligned} \tag{44}$$

Neglecting the second order derivatives in the strain energy function, the constitutive equations remain same except the couple stress–curvature relations, which are given by

$$m_{13} = (8k)\kappa_{13}, \qquad m_{23} = (8k)\kappa_{23}$$

For mixed triangle B (Fig. 6), the strain energy density is obtained from

$$w = \frac{1}{A_c}\left\{W^{OA} + W^{OC} + W^{OE} + W^{OG} + \frac{1}{2}(W^{OB} + W^{OD} + W^{OF} + W^{OH})\right\} \tag{45}$$

with $A_c = 2L^2$.

The strain energy in terms of kinematical variables is given by

$$w = \frac{1}{4L^2}\{(3E'L^2 + 6k)u_{1,1}^2 + (3E'L^2 + 6k)u_{2,2}^2 + (2E'L^2 - 12k)u_{1,1}u_{2,2} + (E'L^2 + 30k)(u_{2,1} - \phi)^2 + (E'L^2 + 30k)(u_{1,2} + \phi)^2 + (2E'L^2 - 12k)(u_{2,1} - \phi)(u_{1,2} + \phi) - 8kL^2\phi_{,1}^2 - 8kL^2\phi_{,2}^2\} \tag{46}$$

and the constitutive relations are given by

$$\begin{aligned}
\sigma_{11} &= \frac{1}{2L^2}\{(3E'L^2+6k)\varepsilon_{11}+(E'L^2-6k)\varepsilon_{22}\}\\
\sigma_{22} &= \frac{1}{2L^2}\{(E'L^2-6k)\varepsilon_{11}+(3E'L^2+6k)\varepsilon_{22}\}\\
\sigma_{12} &= \frac{1}{2L^2}\{(E'L^2+30k)\varepsilon_{12}+(E'L^2-6k)\varepsilon_{21}\}\\
\sigma_{21} &= \frac{1}{2L^2}\{(E'L^2-6k)\varepsilon_{12}+(E'L^2+30k)\varepsilon_{21}\}\\
m_{13} &= (-4k)\kappa_{13}, \qquad m_{23} = (-4k)\kappa_{23}
\end{aligned} \tag{47}$$

The constitutive relations are same when the second order derivatives are ignored except the couple stress–curvature relations which are given by

$$m_{13} = (8k)\kappa_{13}, \qquad m_{23} = (8k)\kappa_{23}$$

4.4. Diamond cell structure

A schematic of the diamond cell structure is shown in Fig. 7. It is made up of isosceles triangles and diagonal square cells. The repeating cell is the square B–C–E–F of area $A_c = 2L^2$. The strain energy density is given in terms of the strain energy of the members as

$$w = \frac{1}{A_c}\left\{\frac{1}{2}(W^{OA}+W^{OD})+W^{OB}+W^{OC}+W^{OE}+W^{OF}\right\} \tag{48}$$

The constitutive equations are derived from the strain energy density function,

$$\begin{aligned}
w = \frac{1}{4L^2}\{&(2E'L^2+12k)u_{1,1}^2+(E'L^2+12k)u_{2,2}^2+(2E'L^2-24k)u_{1,1}u_{2,2}+(E'L^2+24k)(u_{2,1}-\phi)^2\\
&+(E'L^2+12k)(u_{1,2}+\phi)^2+(2E'L^2-24k)(u_{2,1}-\phi)(u_{1,2}+\phi)-6kL^2\phi_{,1}^2-4kL^2\phi_{,2}^2\}
\end{aligned} \tag{49}$$

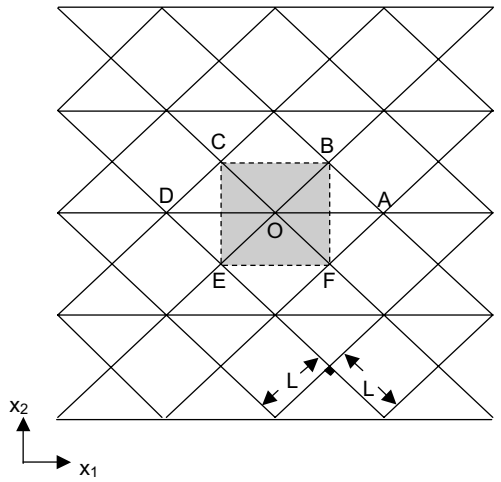

Fig. 7. Schematic of the diamond cell structure.

giving

$$\begin{aligned}
\sigma_{11} &= \frac{1}{2L^2}\{(2E'L^2+12k)\varepsilon_{11}+(E'L^2-12k)\varepsilon_{22}\}\\
\sigma_{22} &= \frac{1}{2L^2}\{(E'L^2-12k)\varepsilon_{11}+(E'L^2+12k)\varepsilon_{22}\}\\
\sigma_{12} &= \frac{1}{2L^2}\{(E'L^2+24k)\varepsilon_{12}+(E'L^2-12k)\varepsilon_{21}\}\\
\sigma_{21} &= \frac{1}{2L^2}\{(E'L^2-12k)\varepsilon_{12}+(E'L^2+12k)\varepsilon_{21}\}\\
m_{13} &= (-3k)\kappa_{13}, \qquad m_{23} = (-2k)\kappa_{23}
\end{aligned} \tag{50}$$

The constitutive relations remain same when the second order derivative terms are ignored except the couple stress–curvature relations, which are given by

$$m_{13} = (6k)\kappa_{13}, \qquad m_{23} = (4k)\kappa_{23}$$

5. Effects of cell wall shear deformation on micropolar elastic constants

So far we have derived the micropolar elastic constants for various cell structures assuming the cell walls behave as Euler–Bernoulli beams. Such an assumption is quite good for typical cellular structures having low relative density as the cell walls then have large aspect ratios. However, if the aspect ratio of the cell walls is small or if the cell wall material has small shear rigidity, the effect of shear deformation must be considered. Furthermore, for purposes of parametric analysis in design, the aspect ratios of the cell walls may be allowed to vary which could lead to cases for which the effects of shear deformation may become important.

The effects of shear deformation can be taken into consideration by treating the cell walls to behave as Timoshenko beams. For Timoshenko beams, the total strain energy (per unit width) of a typical member I–J can be derived as (cf. Eq. (16))

$$W^{\mathrm{IJ}} = \frac{E'}{2}\begin{bmatrix} u_t^{\mathrm{I}} & u_t^{\mathrm{J}} \end{bmatrix}\begin{bmatrix} 1 & -1 \\ -1 & 1 \end{bmatrix}\begin{Bmatrix} u_t^{\mathrm{I}} \\ u_t^{\mathrm{J}} \end{Bmatrix} + \frac{k}{2}\begin{bmatrix} u_n^{\mathrm{I}} & \phi^{\mathrm{I}} & u_n^{\mathrm{J}} & \phi^{\mathrm{J}} \end{bmatrix}\begin{bmatrix} \tilde{s}''/L^2 & \tilde{s}'/L & -\tilde{s}''/L^2 & \tilde{s}'/L \\ \tilde{s}'/L & \tilde{s} & -\tilde{s}'/L & \tilde{s}\tilde{c} \\ -\tilde{s}''/L^2 & -\tilde{s}'/L & \tilde{s}''/L^2 & -\tilde{s}'/L \\ \tilde{s}'/L & \tilde{s}\tilde{c} & -\tilde{s}'/L & \tilde{s} \end{bmatrix}\begin{Bmatrix} u_n^{\mathrm{I}} \\ \phi^{\mathrm{I}} \\ u_n^{\mathrm{J}} \\ \phi^{\mathrm{J}} \end{Bmatrix} \tag{51}$$

where $\tilde{s}'' = 2\tilde{s}'$, $\tilde{s}' = \tilde{s}(1+\tilde{c})$ and $\tilde{s}$ and $\tilde{c}$ are given by

$$\tilde{s} = \frac{4L^2/3 + 4EI/(GA_0)}{L^2/3 + 2EI/(GA_0)}, \qquad \tilde{c} = \frac{2L^2/3 - 4EI/(GA_0)}{4L^2/3 + 4EI/(GA_0)} \tag{52}$$

Here, $I = h^3/12$ and A_0 is the effective cross-sectional area of the member given by $A_0 = \kappa A$, where A is the cross-sectional area of the member and κ is shear correction factor equal to $10(1+\nu)/(12+11\nu)$ for a rectangular cross-section, where ν is the Poisson's ratio (Shames and Dym, 1985). Note that, in the limit as $EI/GA_0 \to 0$, we get $\tilde{s} = 4$ and $\tilde{c} = 1/2$ which corresponds to the Euler–Bernoulli beam theory.

The procedure for obtaining the micropolar elastic constants for various cell structures remains the same as discussed for the Euler–Bernoulli case. Again either of the two approximations of the strain energy function can be made, one ignoring the second order derivative terms all together and the other retaining second order derivative terms that can be integrated by parts to yield first order derivative terms in micro-rotation

Table 1
Micropolar elastic constants for various cell structures considering shear deformation of cell walls (Timoshenko beams)

	Rectangular	Equilateral triangular	Mixed triangle A	Mixed triangle B	Diamond
D_{11}	$E_1'\frac{L_1}{L_2}$	$\frac{\sqrt{3}}{4L^2}(3E'L^2+2k\tilde{s}')$	$\frac{1}{2L^2}(3E'L^2+4k\tilde{s}')$	$\frac{1}{2L^2}(3E'L^2+k\tilde{s}')$	$\frac{1}{2L^2}(2E'L^2+2k\tilde{s}')$
D_{22}	$E_2'\frac{L_2}{L_1}$	$\frac{\sqrt{3}}{4L^2}(3E'L^2+2k\tilde{s}')$	$\frac{1}{2L^2}(3E'L^2+4k\tilde{s}')$	$\frac{1}{2L^2}(3E'L^2+k\tilde{s}')$	$\frac{1}{2L^2}(E'L^2+2k\tilde{s}')$
D_{12}	0	$\frac{\sqrt{3}}{4L^2}(E'L^2-2k\tilde{s}')$	$\frac{1}{2L^2}(E'L^2-4k\tilde{s}')$	$\frac{1}{2L^2}(E'L^2-k\tilde{s}')$	$\frac{1}{2L^2}(E'L^2-2k\tilde{s}')$
D_{33}	$\frac{2k_1\tilde{s}_1'}{L_1L_2}$	$\frac{\sqrt{3}}{4L^2}(E'L^2+6k\tilde{s}')$	$\frac{1}{2L^2}(E'L^2+8k\tilde{s}')$	$\frac{1}{2L^2}(E'L^2+5k\tilde{s}')$	$\frac{1}{2L^2}(E'L^2+4k\tilde{s}')$
D_{44}	$\frac{2k_2\tilde{s}_2'}{L_1L_2}$	$\frac{\sqrt{3}}{4L^2}(E'L^2+6k\tilde{s}')$	$\frac{1}{2L^2}(E'L^2+8k\tilde{s}')$	$\frac{1}{2L^2}(E'L^2+5k\tilde{s}')$	$\frac{1}{2L^2}(E'L^2+2k\tilde{s}')$
D_{34}	0	$\frac{\sqrt{3}}{4L^2}(E'L^2-2k\tilde{s}')$	$\frac{1}{2L^2}(E'L^2-4k\tilde{s}')$	$\frac{1}{2L^2}(E'L^2-k\tilde{s}')$	$\frac{1}{2L^2}(E'L^2-2k\tilde{s}')$
D_{55}	$-\frac{k_1\tilde{s}_1\tilde{c}_1L_1}{L_2}$	$-\sqrt{3}k\tilde{s}\tilde{c}$	$-2k\tilde{s}\tilde{c}$	$-2k\tilde{s}\tilde{c}$	$-\frac{3}{2}k\tilde{s}\tilde{c}$
D_{66}	$-\frac{k_2\tilde{s}_2\tilde{c}_2L_2}{L_1}$	$-\sqrt{3}k\tilde{s}\tilde{c}$	$-2k\tilde{s}\tilde{c}$	$-2k\tilde{s}\tilde{c}$	$-k\tilde{s}\tilde{c}$
D_{55}^*	$\frac{k_1\tilde{s}_1L_1}{L_2}$	$\sqrt{3}k\tilde{s}$	$2k\tilde{s}$	$2k\tilde{s}$	$\frac{3}{2}k\tilde{s}$
D_{66}^*	$\frac{k_2\tilde{s}_2L_2}{L_1}$	$\sqrt{3}k\tilde{s}$	$2k\tilde{s}$	$2k\tilde{s}$	$k\tilde{s}$

in the strain energy function. The constitutive equations for various cell structures can be written compactly as

$$\begin{Bmatrix}\sigma_{11}\\ \sigma_{22}\\ \sigma_{12}\\ \sigma_{21}\\ m_{13}\\ m_{23}\end{Bmatrix}=\begin{bmatrix}D_{11} & D_{12} & 0 & 0 & 0 & 0\\ D_{12} & D_{22} & 0 & 0 & 0 & 0\\ 0 & 0 & D_{33} & D_{34} & 0 & 0\\ 0 & 0 & D_{34} & D_{44} & 0 & 0\\ 0 & 0 & 0 & 0 & D_{55}\text{ or }D_{55}^* & 0\\ 0 & 0 & 0 & 0 & 0 & D_{66}\text{ or }D_{66}^*\end{bmatrix}\begin{Bmatrix}\varepsilon_{11}\\ \varepsilon_{22}\\ \varepsilon_{12}\\ \varepsilon_{21}\\ \kappa_{13}\\ \kappa_{23}\end{Bmatrix} \tag{53}$$

The constants D_{ij} correspond to the case when the second order derivative terms are retained in the strain energy density function after integration by parts. For the case when the second order derivative terms are ignored, the constants D_{ij} relating the stresses σ_{ij} and strains ε_{kl} remain same. However, the moment–curvature relationships now involve constants D_{55}^* and D_{66}^*. The constants for various cell structures are listed in Table 1.

6. Positive definiteness of strain energy with negative micropolar constants

The strain energy density function for a cellular solid modeled with 2-D linear micropolar elasticity can be written in the following form (using Eq. (53))

$$w=\frac{1}{2}(D_{11}\varepsilon_{11}^2+D_{22}\varepsilon_{22}^2+2D_{12}\varepsilon_{11}\varepsilon_{22}+D_{33}\varepsilon_{12}^2+D_{44}\varepsilon_{21}^2+2D_{34}\varepsilon_{12}\varepsilon_{21}+D_{55}\kappa_{13}^2+D_{66}\kappa_{23}^2) \tag{54}$$

with constants D_{ij} for individual cell structures as obtained earlier. As seen from the previous sections, all the micropolar constants are positive when the second and higher order derivative terms in the continuum approximation of the strain energy are ignored. However, when those second order derivative terms are retained that are converted into first order derivatives by integration by parts, we obtained negative D_{55} and D_{66}. This raises some concern regarding the positive definiteness of the strain energy function. Furthermore, the negative value of the constants at first glance appear to violate the bounds on them as derived by Eringen (1968), at least for cell structures that result in isotropic micropolar representation (equilateral triangular). According to the bounds derived by Eringen (1968), these constants should be positive.

Bazant and Christensen (1972) and Bazant and Cedolin (1991), partially addressed the issue of positive definiteness of the strain energy function in the context of square cell structure. They argue that the strain energy of the individual members of the unit cell is positive. Hence their summation and continuous approximation must be positive. Even though this argument provides sound justification, it fails to address why these constants should violate the bounds derived for micropolar elastic solids in the isotropic case. We provide some explanation for this apparently paradoxical result.

Both the issues, namely positive definiteness of strain energy function and positive micropolar constants, are related. The bounds on isotropic micropolar constants were derived by Eringen (1968) considering the continuum to be purely local. In such a case, the strains ε and curvature κ can be varied independently for an infinitesimal material element. This would imply positive definite strain energy function only for positive D_{55} and D_{66} (cf. Eq. (54)). However, when representing the cellular microstructure with an equivalent micropolar continuum, we have a limited non-locality. The continuum material element cannot be less than the characteristic cell size over which the continuum strain energy density is defined. The stresses and couple stresses are assumed to act on the surface of the material element whereas the displacement and micro-rotation correspond to the centroid of the element, the point about which the displacement and micro-rotation are expanded in the Taylor series representation. The strain energy function averaged over this volume of element should be positive definite and not the pointwise local strain energy function. Thus coefficients D_{55} and D_{66} can be negative as long as the strain energy density function integrated over the periodic unit cell is positive definite.

7. Finite element implementation

The finite element implementation of micropolar elasticity is straightforward. The starting point is the principle of virtual work (assuming zero body forces and moments) given by

$$\int_{\Omega} (\sigma_{ij}\,\delta\varepsilon_{ij} + m_{ij}\,\delta\kappa_{ij})\,\mathrm{d}V = \int_{\partial\Omega} (T_i\,\delta u_i + Q_i\,\delta\phi_i)\,\mathrm{d}A \tag{55}$$

where T_i and Q_i are applied surface traction and surface moment vectors, respectively. Substituting Eqs. (3) and (4) in Eq. (55), we get

$$\int_{\Omega} (\sigma_{ij}\,\delta u_{j,i} - \varepsilon_{ijk}\sigma_{ij}\,\delta\phi_k + m_{ij}\,\delta\phi_{j,i})\,\mathrm{d}V = \int_{\partial\Omega} (T_i\,\delta u_i + Q_i\,\delta\phi_i)\,\mathrm{d}A \tag{56}$$

where δu_i is virtual displacement vector and $\delta\phi_i$ is virtual micro-rotation vector. The principle of virtual work is valid for the entire domain as well as any sub-domain (finite element). We approximate the displacement and micro-rotation field over the element from the corresponding nodal values using interpolation functions as

$$\{u\} = [N^u]\{d^u\}, \qquad \{\phi\} = [N^\phi]\{d^\phi\} \tag{57}$$

Substituting the approximate displacement and micro-rotational fields in to the discretized form of the principle of the virtual work (Eq. (56)), we obtain the element level equation as

$$[K]^{\mathrm{e}}\{d\}^{\mathrm{e}} = \{f\}^{\mathrm{e}} \tag{58}$$

The global system of algebraic equations can be obtained using the standard finite element assembly techniques. The assembly of the element equations into a global system of equation enforces the continuity of displacement and micro-rotation components between the elements. The global finite element equations can be solved after imposing appropriate kinematic boundary conditions on the displacement boundary

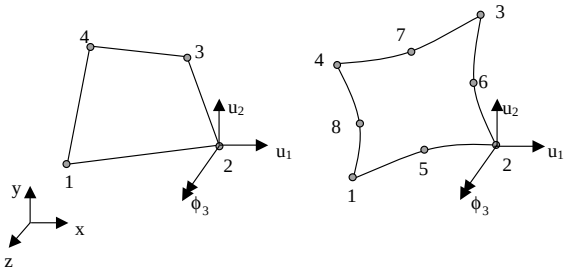

Fig. 8. Linear and quadratic micropolar elements.

of the domain. This involves prescribing the appropriate nodal displacement and micro-rotation components at a node on the displacement boundary.

The finite element equations developed in the foregoing are implemented in ABAQUS finite element program (ABAQUS, Inc., 2002) as a user-defined element. Planar four-node and eight-node isoparametric elements are developed with the micropolar theory. Each node has three degrees of freedom—two in-plane displacement components, u_1 and u_2, and an in-plane micro-rotation component, ϕ_3 (Fig. 8).

Both the displacement and micro-rotation components are interpolated using same shape functions, which for the four-node element are given by

$$\begin{aligned} N_1^e &= (1-\xi)(1-\eta)/4; \qquad N_2^e = (1+\xi)(1-\eta)/4 \\ N_3^e &= (1+\xi)(1+\eta)/4; \qquad N_4^e = (1-\xi)(1+\eta)/4 \end{aligned} \tag{59}$$

on the other hand, the eight-node element uses quadratic shape functions given by

$$\begin{aligned} N_1^e &= \xi\eta(1-\xi)(1-\eta)/4; \qquad N_2^e = -\xi\eta(1+\xi)(1-\eta)/4 \\ N_3^e &= \xi\eta(1+\xi)(1+\eta)/4; \qquad N_4^e = -\xi\eta(1-\xi)(1+\eta)/4 \\ N_5^e &= -\eta(1-\xi^2)(1-\eta)/2; \qquad N_6^e = \xi(1+\xi)(1-\eta^2)/2 \\ N_7^e &= \eta(1-\xi^2)(1+\eta)/2; \qquad N_8^e = -\xi(1-\xi)(1-\eta^2)/2 \end{aligned} \tag{60}$$

where ξ and η are the natural coordinates. Furthermore, full Gauss integration is used for both the elements.

The element can be used in conjunction with either homogeneous isotropic micropolar solid (without an underlying cell structure) or with cellular material using constants derived in Sections 4 and 5. The element formulation is verified by solving the problem of stress concentration factor around a circular notch in a large plate made of homogeneous isotropic micropolar solid. The results from the finite element simulations are compared with the known analytical solution for a circular notch in an infinite plate for a homogeneous isotropic micropolar elastic solid (Kaloni and Ariman, 1967). The results from the finite element solution match the analytical solution (in the limit of large plate dimension to notch radius ratio), thus verifying the micropolar finite element implementation.

8. Comparison of generalized continuum with "exact" discrete models

In order to assess the generalized continuum formulation of cellular materials developed in this paper, we compare the results with the "exact" discrete simulations. The discrete simulations are performed using finite element analysis of the cell structure with the cell walls modeled using beam elements.

For this study, we choose a model problem of indentation of a rectangular block. The bottom edge of the block is assumed to be fixed (i.e., $u_1 = u_2 = \phi = 0$) while the sides are traction free, i.e., both stress and couple stress tractions are zero (cf. Eq. (8)). The top surface is also traction free except for a point force applied at its center (Fig. 9). The cell wall material is assumed to be isotropic linear elastic defined by Young's modulus of 120 GPa and Poisson's ratio of 0.3. The characteristic length L of various cell structures is taken as 2.0 mm. The relative density of the cellular material is taken as 0.1 for all the cell structures. As the characteristic cell wall length and relative density of the cellular material is fixed, the cell wall thickness varies for different cell topologies.

The discrete analysis is carried out using ABAQUS finite element program. The cell wall is modeled using Euler–Bernoulli beam elements. Each segment of the cell wall is modeled using three beam elements along its length.

The generalized continuum modeling is performed using the finite element approach as well. The domain is discretized using four-noded quadrilateral user element developed in Section 7. The continuum model is described by the micropolar elastic constants of each cell topology developed in Section 4. The cell walls for this model problem are slender and hence the effect of shear deformation on the micropolar constants is not considered.

For the square cell topology, both sets of constants are used in the simulations—one obtained by ignoring the second order derivative terms in the strain energy density function and the other obtained by retaining this term after integration by parts (see Section 4). The relative size of the finite element mesh with respect to the characteristic cell size is varied in order to study its effect on the overall solution. Fig. 10(a)–(c) present the displacement and micro-rotation of the top edge obtained from the continuum and discrete models. The number of elements used in the continuum model is indicated in the figure legends. Note that 50×25 continuum elements correspond to one cell per finite element, 30×15 elements correspond to four cells, 20×10 elements correspond to nine cells and 10×5 elements correspond to 25 cells. It is noted that the accuracy of the finite element solution based on micropolar theory is poor in the vicinity of the applied point load due to very large gradients of stresses and strains associated with that point. Mesh refinement in this region can only be carried out until the element size is of the same order as the characteristic cell size. The intrinsic limitation of micropolar continuum modeling in the regions of large gradients is due to the fact that such gradients have not been accounted for in deriving the micropolar elastic constants for various periodic cell structures. Higher order micropolar models would be necessary for this purpose.

The solutions for the square cell topology presented in the foregoing display some interesting features. The solutions obtained from the continuum analysis utilizing constants obtained from the two approaches are similar when the finite element size contains four or more cells. The solution using the approach that considers second order derivative terms in the strain energy function leads to oscillations in displacement and micro-rotation when the element size is comparable to the cell size. By using a suitably large element, the results from the continuum analysis compare reasonably well with the discrete solutions. Of course, as

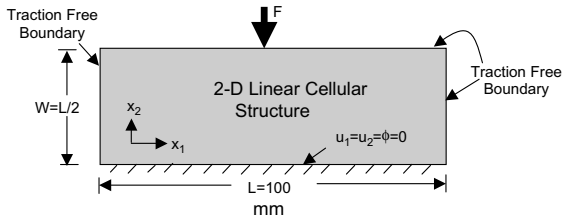

Fig. 9. Elastic indentation of a rectangular block made of linear cellular alloys.

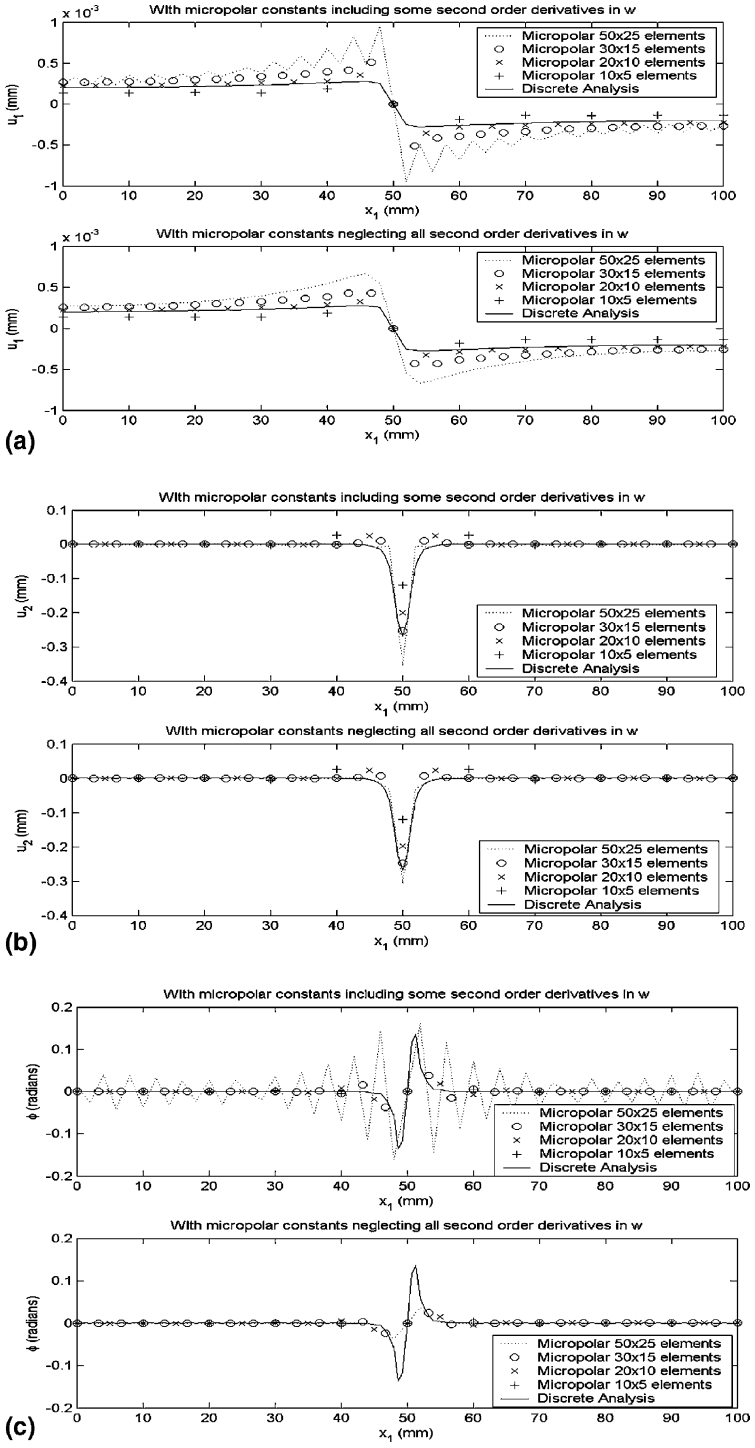

Fig. 10. Comparison of micropolar and discrete analysis for square cell structure: (a) displacement u_1 of the top surface, (b) displacement u_2 of the top surface, (c) micro-rotation ϕ of the top surface.

expected, the behavior near the point of applied loading is not captured very accurately due to neglect of stress and strain gradients in the derivation of micropolar constants for periodic unit cells.

The continuum simulations for the remaining cell topologies are conducted using 20×10 elements to discretize the rectangular domain. These results are presented in Figs. 11–14 for equilateral triangular, mixed triangle-A, mixed triangle-B and diamond cell topologies, respectively. Again both methods of obtaining micropolar constants are compared with "exact" discrete simulations in terms of displacements and micro-rotation on the top edge.

The results show that the continuum simulations capture the overall behavior in reasonably accurate manner for the square, equilateral triangular, mixed triangles A and B and, to a somewhat lesser extent, the diamond cell structures.

9. Application of continuum modeling—comparison of cell topologies

Generalized continuum modeling of cellular structures is advantageous compared to discrete modeling for some applications as it is computationally more efficient. Furthermore, complex boundary value problems can be easily handled using the generalized continuum approach. One of the applications of the continuum approach is to compare different cell topologies for design of structures of dimensions large compare to cell size. As an illustration, we consider the problem of stress concentration factor around a circular notch in a 2-D cellular material.

The geometry considered for the analysis, along with the finite element mesh and boundary conditions, is shown in Fig. 15. Due to symmetry, only a quarter of the plate is analyzed. On edge PA, displacement in the y-direction and the micro-rotation ϕ are constrained, whereas on edge QC displacement in the x-direction and the micro-rotation are constrained. The edge of the notch and the right edge are traction free boundary with both stress and couple stress tractions zero (cf. Eq. (8)). On the top edge BC, displacement in the global y-direction is prescribed and the corresponding stress $\sigma_{22}^{\text{Applied}}$ is obtained from the simulation. Other components of the stress and couple stress tractions on this edge are zero, i.e., σ_{21} and m_{23} are zero on the top edge. The cell wall material is taken as isotropic linear elastic with Young's modulus 120 GPa and Poisson's ratio 0.3. The relative density of the cellular material is taken as 0.1 and the characteristic cell wall length, L, is taken as 2 mm for all cell topologies considered. Eight-noded quadratic elements

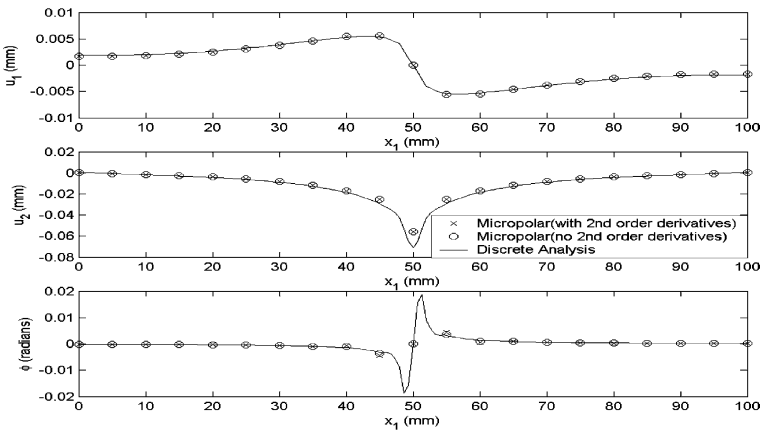

Fig. 11. Displacements and micro-rotation of the top edge for equilateral triangular cell structure.

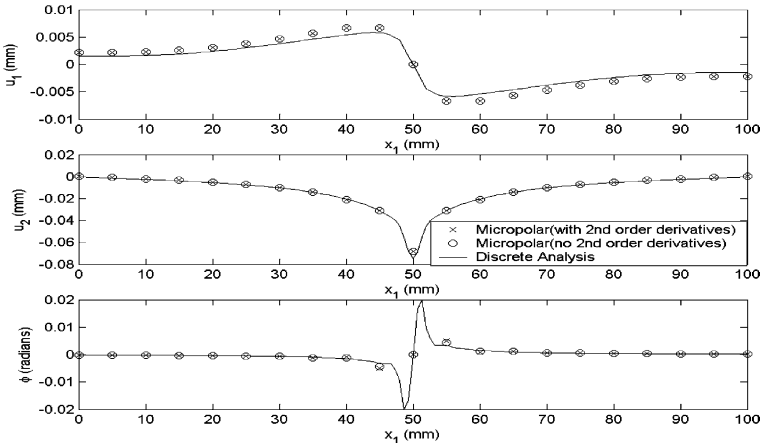

Fig. 12. Displacements and micro-rotation of the top edge for mixed triangle-A cell structure.

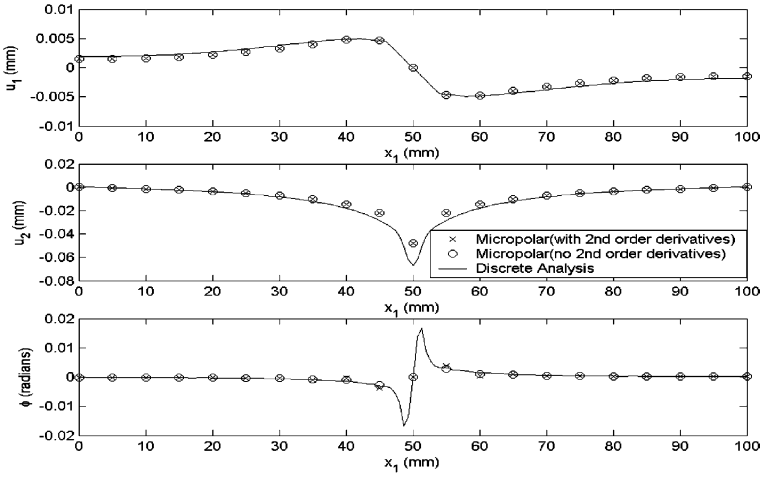

Fig. 13. Displacements and micro-rotation of the top edge for mixed triangle-B cell structure.

are used in this study. The mesh is such that the minimum element size is 5 mm. This choice is based on two considerations: first the mesh should be fine enough to capture the gradients in solution due to the notch and secondly, the element size should not be less than the characteristic cell dimension (cell wall length); otherwise it is not representative of the underlying cell structure. The micropolar elastic constants chosen are those obtained by neglecting the second order derivative terms in the strain energy functions.

The stress concentration factor, defined as $\mathrm{SCF} = \sigma_{22}^{\mathrm{P}}/\sigma_{22}^{\mathrm{Applied}}$, is shown in Fig. 16 for various cell topologies. The cells are oriented such that their local orientation $x_1 - x_2$ (as shown in Figs. 3–7 of Section 4) coincides with the global x and y directions shown in Fig. 15. Fig. 16 shows that the square cell structure has the highest stress concentration factor and the diamond cell structure has the lowest stress concentration factor. The high value of stress concentration factor for square cell structure has also been obtained by Adachi et al. (1998). In conclusion, the diamond cell structure is the best choice amongst all the cells considered for this particular loading condition and cell orientation when the design is to be based solely on the stress concentration factor.

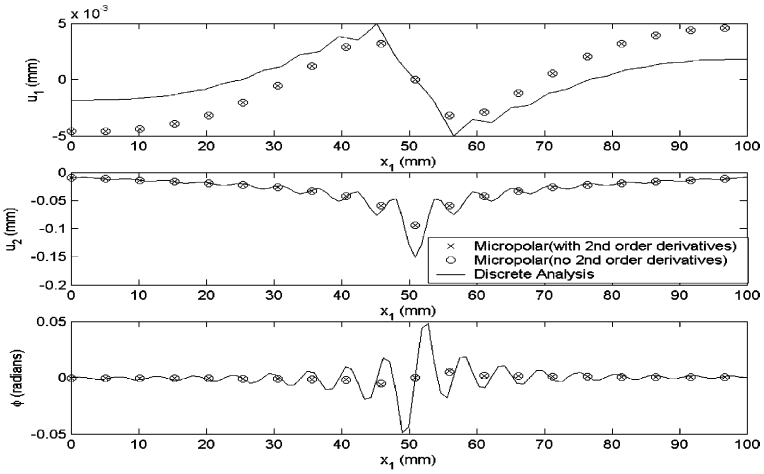

Fig. 14. Displacements and micro-rotation of the top edge for diamond cell structure.

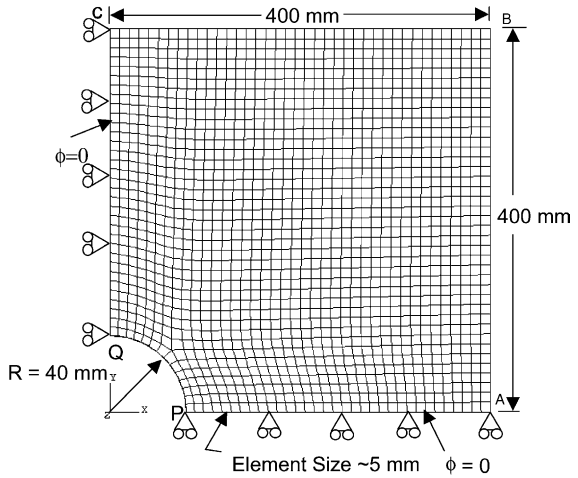

Fig. 15. Continuum modeling of circular notch in a plate made of various cell structures.

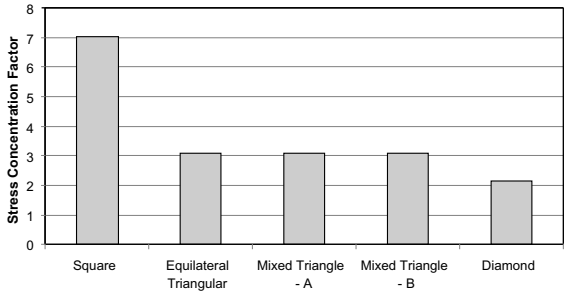

Fig. 16. Stress concentration factor for various cell structures.

10. Conclusions

A strain energy-based approach is used to derive micropolar elastic constants for various 2-D periodic cell structures namely, rectangular, equilateral triangular, mixed triangle and diamond. All of these cell structures have the common characteristic that a single joint can be identified as defining a periodic unit cell. Two sets of constants are obtained by considering different order of approximations in the continuum representation of the strain energy function. Furthermore, micropolar constants considering the effect of shear deformation of cell walls are derived. A micropolar finite element is developed to analyze and compare various cell structures.

Elastic indentation of a rectangular block by a point force is considered to compare the continuum micropolar theory and the "exact" discrete analysis. The solutions from the micropolar continuum approach are found to be of reasonable accuracy for rectangular, equilateral triangular, mixed triangle and diamond structures. The analysis also illustrates that the two sets of micropolar constants result in similar response as long as the finite element size is greater than the characteristic cell size.

To illustrate the utility of the continuum modeling in design selection, a problem of stress concentration factor around a circular notch is considered. For the considered cell dimensions and orientation, it is found that square cell structure leads to highest stress concentration factor, whereas the diamond cell structure results in the lowest stress concentration factor.

It is clear that the approximate generalized continuum approach to model cellular structures has an advantage over discrete modeling especially for design selection exercises involving various cell topologies and complex domains. However, the approach is limited to periodic cell structures that contain a single representative joint within its periodic unit cell as well as to problems where the gradients of stresses and strains are not excessive. Particular attention must be paid in meshing the domain so that the element size does not reduce below the characteristic cell size. The two conflicting requirements that the element size should be small for capturing large gradients but larger than the characteristic cell size cannot be resolved using the local micropolar theory presented here. Further research is underway to address this issue as well as a related problem of continuum modeling of non-periodic (i.e., graded) cell structures.

Acknowledgment

The authors gratefully acknowledge the support of the Carter N. Paden, Jr. Distinguished Chair in Metals Processing.

References

ABAQUS, Inc., 2002. User's Manual, Version 6.3-1. Pawtucket, RI.

Adachi, T., Tomita, Y., Tanaka, M., 1998. Computational simulation of deformation behavior of 2D-lattice continuum. International Journal of Mechanical Science 40 (9), 857–866.

Askar, A., Cakmak, A.S., 1968. A structural model of micropolar continuum. International Journal of Engineering Science 6, 583–589.

Banks, C.B., Sokolowski, M., 1968. On certain two-dimensional applications of the couple stress theory. International Journal of Solids and Structures 4, 15–29.

Bazant, Z.P., 1971. Micropolar medium as model for buckling of grid frameworks. In: Developments in Mechanics, Proceedings of the 12th Midwestern Mechanics Conference, vol. 6. pp. 587–594.

Bazant, Z.P., Cedolin, L., 1991. Stability of Structures. Oxford University Press, New York pp. 129–138.

Bazant, Z.P., Christensen, M., 1972. Analogy between micropolar continuum and grid frameworks under initial stress. International Journal of Solids and Structures 8, 327–346.

Chen, J.Y., Huang, Y., Ortiz, M., 1998. Fracture analysis of cellular materials: a strain gradient model. Journal of the Mechanics and Physics of Solids 46 (5), 789–828.

Cochran, J.K., Lee, K.J., McDowell, D.L., Sanders, T.H., Church, B., Clark, J., Dempsey, B., Hayes, A., Hurysz, K., McCoy, T., Nadler, J., Oh, R., Seay, W., Shapiro, B., 2000. Low density monolithic honeycombs by thermal chemical processing. In: Proceedings of the 4th Conference on Aerospace Materials, Processes, and Environmental Technology, September 18–20, 2000, Huntsville, AL.

Cosserat, E., Cosserat, F., 1909. Théorie des Corps Déformables. Hermann, Paris.

Deshpande, V.S., Ashby, M.F., Fleck, N.A., 2001. Foam topology: bending versus stretching dominated architectures. Acta Materialia 49, 1035–1040.

Eringen, A.C., 1966. Linear theory of micropolar elasticity. Journal of Mathematics and Mechanics 15 (6), 909–923.

Eringen, A.C., 1968. Theory of micropolar elasticity. In: Liebowitz, H. (Ed.), Fracture—An Advanced Treatise, Vol. II: Mathematical Fundamentals. Academic Press, New York.

Eringen, A.C., 1999. Microcontinuum Field Theories I: Foundations and Solids. Springer, New York.

Evans, A.G., Hutchinson, J.W., Ashby, M.F., 1998. Multifunctionality of cellular metal systems. Progress in Materials Science 43, 171–221.

Evans, A.G., Hutchinson, J.W., Fleck, N.A., Ashby, M.F., Wadley, H.N.G., 2001. The topological design of multifunctional cellular metals. Progress in Materials Science 46, 309–327.

Gibson, L.J., Ashby, M.F., 1997. Cellular Solids, second ed. Cambridge University Press, Cambridge, UK.

Kaloni, P.N., Ariman, T., 1967. Stress concentration effects in micropolar elasticity. Journal of Applied Mathematics and Physics (ZAMP) 18, 136–141.

Kumar, R.S., McDowell, D.L., in preparation.

Nowacki, W., 1986. Theory of Asymmetric Elasticity. Pergamon Press, New York.

Perano, K.J., 1983. Application of micropolar elasticity to the finite element continuum analysis of articulated structures. Ph.D. Dissertation, University of California, Davis, USA.

Shames, I.H., Dym, C.L., 1985. Energy and Finite Element Methods in Structural Mechanics. Hemisphere Publishing Corporation, New York p. 200.

Wang, A.J., McDowell, D.L., 2004. In-plane stiffness and yield strength of periodic metal honeycombs. ASME Journal of Engineering Materials and Technology 126, 137–156.

Wang, A.J., McDowell, D.L., in press. Yield surfaces of various periodic metal honeycombs at intermediate relative density. International Journal of Plasticity.

Wang, X.L., Stronge, W.J., 1999. Micropolar theory for two-dimensional stresses in elastic honeycomb. Proceedings of the Royal Society of London A 455, 2091–2116.

Warren, W.E., Byskov, E., 2002. Three-fold symmetry restrictions on two-dimensional micropolar materials. European Journal of Mechanics A/Solids 21, 779–792.